nated from further analysis because they were significantly more active preceding saccades to T2 than to T1. Thus, our final database consisted of 96 choice-predicting SC neurons.
10. K. H. Britten, M. N. Shadlen, W. T. Newsome, J. A. Movshon, *J. Neurosci.* **12**, 4745 (1992).
11. J. D. Roitman and M. N. Shadlen, *Soc. Neurosci. Abstr.* **24**, 262 (1998).
12. For each cell isolated, we presented 6 to 15 repetitions of a 51.2% coherence stimulus of 1- to 2-s duration, moving either toward or away from the movement field.
13. In saccade trials, a single target was illuminated contralateral to the cell's movement field 300 ms after the monkey fixated. This event indicated to the monkey that a saccade to the target (within 500 ms of fixation point disappearance) would be required in order to obtain a reward. Saccade and passive fixation trials were randomly interleaved.
14. Direction tuning curves were parameterized by least-squares fits of Gaussian functions to mean firing rates according to the following equation:

$$\text{firing\_rate} = \text{baseline} + \text{amplitude} \times \exp[-(\text{motion\_dir} - \text{pref\_dir})^2/(2 \times \text{width}^2)]$$

15. N. P. Bichot, J. D. Schall, K. G. Thompson, *Nature* **381**, 697 (1996).
16. This monkey was trained to perform a direction discrimination task in which the mapping between the direction of visual motion and the operant saccade vector varied substantially from trial to trial. Direction selectivity was measured during a passive fixation task, as it was for the other monkeys in this study. Only 5 of 35 intermediate-layer neurons exhibited significant direction selectivity (Mann-Whitney U-test: $P < 0.05$). Data from this animal will be described fully elsewhere.
17. We performed this analysis separately for each motion strength using only correctly answered trials. Time was quantized in nonoverlapping 100-ms bins spanning the trial. We calculated normalized activity for each cell by counting the number of spikes in each time bin and dividing by the maximum mean spike count (mean across trials, maximum across motion strengths and time bins). Normalized spike counts were first pooled across cells and then segregated with respect to the monkey's psychophysical decision. For each time bin, we calculated an ROC (receiver operating characteristic) curve from the two distributions of spike counts and integrated its area. This metric can be interpreted as the probability with which an ideal observer could predict the monkey's choice on the basis of the normalized spike count in that time bin.
18. D. M. Green and J. A. Swets, *Signal Detection Theory and Psychophysics* (Wiley, New York, 1966).
19. M. N. Shadlen and J. N. Kim, *Nature Neurosci.* **2**, 176 (1998).
20. M. Shadlen and W. Newsome, *Proc. Natl. Acad. Sci. U.S.A.* **93**, 628 (1996).
21. For each of the five 100-ms-long epochs preceding the onset of the visual stimulus, we assigned spike counts from T1 choice trials and T2 choice trials randomly to two distributions. We then calculated the ROC curve for the two distributions and integrated its area. This procedure was repeated 5000 times to estimate the distribution of ROC areas that would be expected by chance. The cited *P* value indicates the proportion of the 5000 iterations in which the ROC value computed from the randomized data equaled or exceeded the ROC value computed from the experimental (nonrandomized) data.
22. We suggest that the monkey enters some trials favoring one target over the other, and that this bias is reflected in small firing rate differences before onset of the visual stimulus. When the motion coherence is high, the direction of stimulus motion largely determines the monkey's choices, overriding the weak bias that exists entering the trial. Because the direction of stimulus motion is chosen randomly, trials in which the monkey is biased toward T1 or T2 have an equal probability of resulting in a T1 or T2 decision, and little or no differential activity is apparent when the trials are subsequently sorted and analyzed according to decision outcome. At 0% coherence, however, the monkey tends to choose in the direction of the bias because there is no directional signal to override the bias. Thus, the small differences in neural activity associated with the bias (before stimulus onset) become associated with the decision and are apparent when the trials are sorted and analyzed according to decision outcome.
23. All coherences were averaged together for these analyses. Latency was defined as the time from stimulus onset until predictive activity exceeded the baseline level by three standard deviations. Time was quantized in 10-ms bins for this analysis because the difference in latency between the two groups was only 30 ms. For the time course analysis we calculated the time to reach half of the maximum predictive activity obtained during the stimulus presentation. This time differed between the two groups by 300 ms. Distributions of both statistics under the null hypothesis were generated by randomly reassigning the cells to two groups 2000 times, calculating the value of the statistic for both groups, and recording the difference. The cited *P* value is the proportion of differences greater than or equal to the actual difference obtained from the nonrandomized data.
24. M. A. Basso and R. H. Wurtz, *J. Neurosci.* **18**, 7519 (1998).
25. J. W. Gnadt and R. A. Andersen, *Exp. Brain Res.* **70**, 216 (1988).
26. J. Schall and D. Hanes, *Nature* **366**, 467 (1993).
27. P. Mazzoni, R. Bracewell, S. Barash, R. Andersen, *J. Neurophysiol.* **76**, 1439 (1996).
28. D. A. Robinson, *IEEE Trans. Biomed. Eng.* **10**, 137 (1963).
29. We thank C. Barberini, G. DeAngelis, J. Liu, J. Nichols, and M. Shadlen for critical feedback and comments on the manuscript. All experimental procedures and care of the animals were carried out in compliance with guidelines established by NIH and approved by the Institutional Animal Care and Use Committee of Stanford University. Supported by the National Eye Institute (grant 05603) and by the Human Frontiers Science Research Program. G.D.H. was supported by a predoctoral fellowship from the Office of Naval Research and by training grant 5T32NH17047-17 from NIH. W.T.N. is an Investigator with the Howard Hughes Medical Institute.

9 November 1998; accepted 8 April 1999

Interaction of RAFT1 with Gephyrin Required for Rapamycin-Sensitive Signaling

David M. Sabatini,[1*] Roxanne K. Barrow,[1] Seth Blackshaw,[1] Patrick E. Burnett,[1] Michael M. Lai,[1] Michael E. Field,[1] Ben A. Bahr,[2] Joachim Kirsch,[3] Heinrich Betz,[3] Solomon H. Snyder[1†]

RAFT1 (rapamycin and FKBP12 target 1; also called FRAP or mTOR) is a member of the ATM (ataxia telangiectasia mutated)–related family of proteins and functions as the in vivo mediator of the effects of the immunosuppressant rapamycin and as an important regulator of messenger RNA translation. In mammalian cells RAFT1 interacted with gephyrin, a widely expressed protein necessary for the clustering of glycine receptors at the cell membrane of neurons. RAFT1 mutants that could not associate with gephyrin failed to signal to downstream molecules, including the p70 ribosomal S6 kinase and the eIF-4E binding protein, 4E-BP1. The interaction with gephyrin ascribes a function to the large amino-terminal region of an ATM-related protein and reveals a role in signal transduction for the clustering protein gephyrin.

Proteins of the ATM family participate in cell cycle progression by linking signals from growth factor receptors and internal checkpoints to the cell cycle machinery. These cell cycle regulators are members of the kinase superfamily and include the gene product of the ataxia telangiectasia locus (*ATM*), the catalytic subunit of the DNA-activated protein kinase (DNA-PKcs), RAFT1 or FRAP, and the products of the yeast genes *TOR1*, *TOR2*, and *TEL1* (*1*).

RAFT1 and its yeast homologs, the TOR proteins, are the in vivo targets for the complex of rapamycin with its intracellular receptor, FKBP12. Rapamycin is a potent immunosuppressant that prevents progression through the G_1 phase of the cell cycle in various cell types, including T lymphocytes and budding yeast (*2*). The effects of rapamycin point to a role for RAFT1 and the TORs in cell cycle regulation, and increasing evidence indicates that they participate in mitogen-stimulated signaling pathways that control mRNA translation. In mammalian cells RAFT1 controls the rapamycin-sensitive phosphorylation of at least two transla-

[1]The Johns Hopkins University School of Medicine, Department of Neuroscience, 725 North Wolfe Street, Baltimore, MD 21205, USA. [2]Department of Pharmaceutical Sciences, University of Connecticut, Storrs, CT 06269, USA. [3]Department of Neurochemistry, Max Planck Institute for Brain Research, Deutschordenstrasse 46, 60528 Frankfurt/Main, Germany.

*Present address: Whitehead Institute for Biomedical Research, 9 Cambridge Center, Cambridge, MA 02142, USA.

†To whom correspondence should be addressed. E-mail: ssnyder@jhmi.edu

tional regulators: the p70 ribosomal S6 kinase ($p70^{S6k}$) and 4E-BP1, an inhibitor of the cap binding protein eIF-4E (*3*, *4*). In yeast, TOR function is necessary for initiation of mRNA translation and may contribute to a checkpoint that prevents cell cycle progression in the absence of nutrients (*5*).

All ATM-related proteins are large (greater than 200 kD) and have a COOH-terminal region with similarity to the catalytic domains of phosphoinositide 3- and 4-kinases (*6*). Despite this similarity, RAFT1 and related proteins appear to be protein kinases, and RAFT1 immunoprecipitates directly phosphorylate $p70^{S6k}$ (*7*) and 4E-BP1 in vitro (*4*, *7*).

To identify proteins that may interact with the first 2000 residues of RAFT1, we arbitrarily subdivided this region and used each part individually as bait in a yeast two-hybrid screen of a rat hippocampal expression library (*8*). Amino acids 944 to 1338 of RAFT1 interacted with gephyrin, a tubulin-binding protein necessary for the postsynaptic clustering of glycine receptors in spinal cord neurons (*9*). Residues 1010 to 1128 are the smallest part of RAFT1 that interacted with gephyrin in the yeast two-hybrid assay and represent the minimal gephyrin-binding domain (GBD) of RAFT1 (Fig. 1A). Alignment of the 118–amino acid GBD and the intracellular loop of the β subunit of the glycine receptor revealed that residues 1017 to 1046 of RAFT1 share 45% sequence similarity to residues 405 to 435 of the glycine receptor (Fig. 1B). This is the same region of the receptor that interacts with gephyrin (*10*). By mutating several of the residues conserved between RAFT1 and the glycine receptor we created RAFT1 mutants that do not interact with gephyrin (RAFT1 I1034K and IV1034-5KR) or that show decreased binding to gephyrin relative to that of the wild-type protein (RAFT1 I1034A) (Fig. 1B).

We used an in vitro binding assay to determine that full-length RAFT1 also interacts with gephyrin (*11*). Endogenous RAFT1 from detergent lysates of human embryonic kidney (HEK293) cells bound to a glutathione *S*-transferase (GST)–gephyrin affinity resin but not to one made with GST alone (Fig. 2A). The gephyrin-RAFT1 interaction was unaffected by the addition of 10 nM rapamycin to the cell lysates. We also expressed gephyrin in HEK293 cells with wild-type RAFT1 or variants incorporating mutations that reduced or eliminated the GBD-gephyrin interaction in yeast (*12*). Antibodies to gephyrin coimmunoprecipitated wild-type RAFT1 but not the I1034K or IV1034-5KR RAFT1 mutants (Fig. 2B). Similarly, RAFT1 I1034A, which retains partial binding to gephyrin in yeast, coimmunoprecipitated with gephyrin but in smaller amounts than the wild-type protein (Fig. 2B). Thus, RAFT1 interacts with gephyrin in HEK293 cells, and point mutations in the GBD reduce or eliminate the interaction in yeast and mammalian cells.

All tissues examined contained RAFT1 and gephyrin, including HEK293 cells, which express full-length RAFT1 and the 93-kD form of gephyrin (*13*). In rat embryos RAFT1 and gephyrin mRNAs are widely expressed, with the largest amounts found in the developing central nervous system, kidney, thymus, and small intestine (*14*). In subcellular fractions (Fig. 3A) of rat brain both RAFT1 and gephyrin were abundant in the LP2 fraction, which is highly enriched in synaptic vesicles and presynaptic membranes (*15*). RAFT1 was not detected in the soluble fraction of synaptosomes (LS2) whereas gephyrin was present in small amounts (Fig. 3A).

We examined whether gephyrin might contribute to the intracellular localization of RAFT1 as it does for the glycine receptor (*9*). In HeLa cell subcellular fractions, as in the brain (Fig. 3A), RAFT1 was enriched in cellular membranes (Fig. 3B). Immunofluorescence staining of HeLa cells with an antibody to RAFT1 revealed a fine punctate pattern in the cytoplasm that is not characteristic of any particular subcellular compartment (Fig. 3C) but is similar in appearance to the cytoplasmic localization of the related protein ATM (*16*). Overexpression in HeLa cells of the

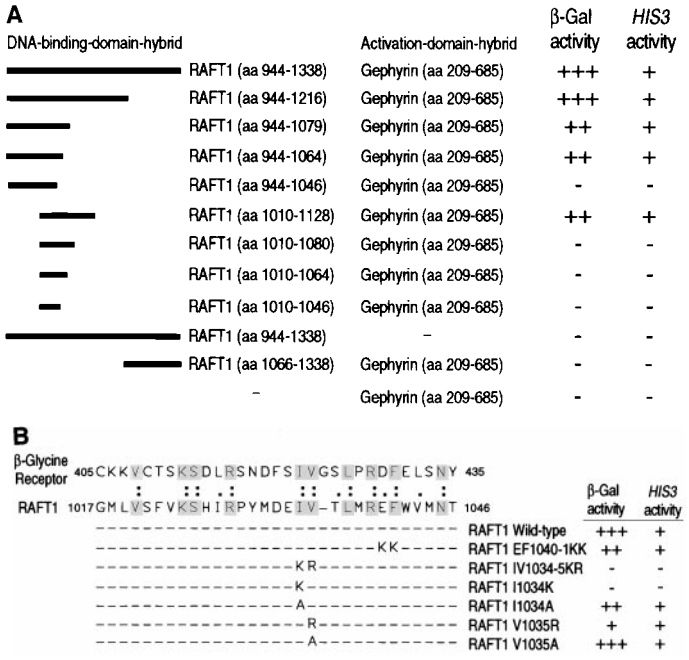

Fig. 1. Specific interaction between gephyrin and amino acids (aa) 944 to 1338 of RAFT1. (**A**) Interaction of indicated RAFT1 fragments with gephyrin in yeast two-hybrid system (*8*). The results were scored as follows: for β-Gal: +++, blue color in <15 min; ++, blue color in 15 to 45 min; +, blue color in 45 to 120 min; –, no blue color in <24 hours. For *HIS3*: +, growth or –, no growth on histidine-free media. (**B**) Residues 1017 to 1046 of RAFT1 are 45% similar to residues 405 to 435 of the β-chain of the glycine receptor (*20*). Isoleucine 1034 is critical for the RAFT1-gephyrin interaction; replacement with lysine or alanine abolishes or reduces, respectively, the association (*8*).

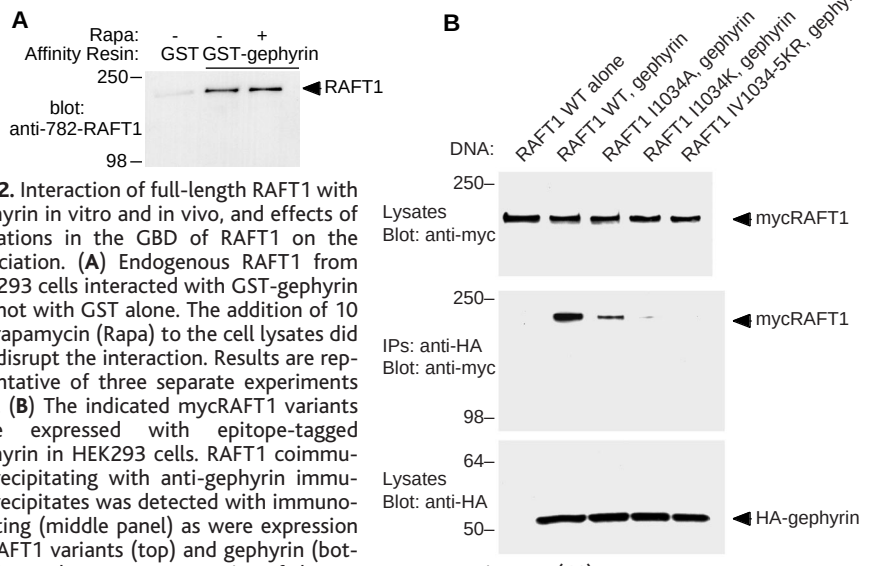

Fig. 2. Interaction of full-length RAFT1 with gephyrin in vitro and in vivo, and effects of mutations in the GBD of RAFT1 on the association. (**A**) Endogenous RAFT1 from HEK293 cells interacted with GST-gephyrin but not with GST alone. The addition of 10 nM rapamycin (Rapa) to the cell lysates did not disrupt the interaction. Results are representative of three separate experiments (*11*). (**B**) The indicated mycRAFT1 variants were expressed with epitope-tagged gephyrin in HEK293 cells. RAFT1 coimmunoprecipitating with anti-gephyrin immunoprecipitates was detected with immunoblotting (middle panel) as were expression of RAFT1 variants (top) and gephyrin (bottom). Results are representative of three separate experiments (*12*).

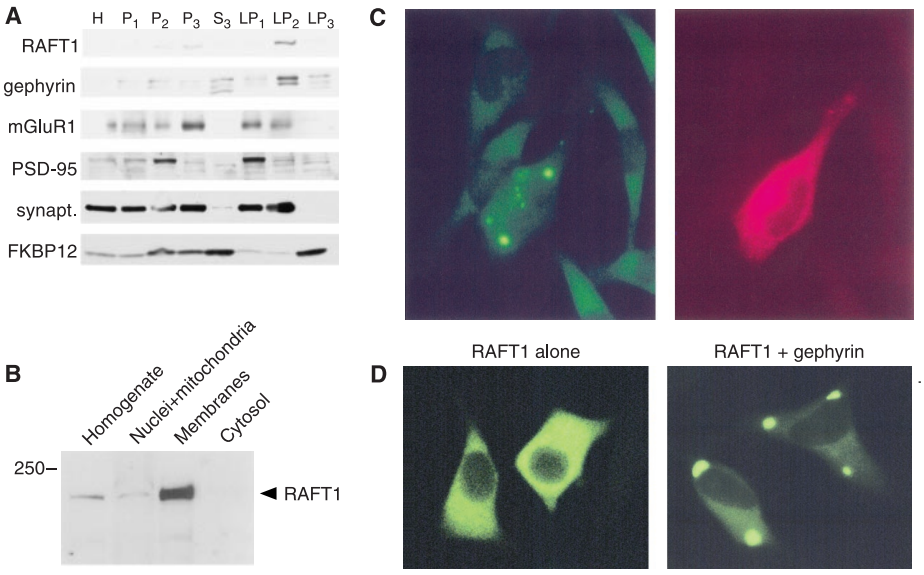

Fig. 3. Subcellular localization of RAFT1 and gephyrin and effects of overexpression of the RAFT1 GBD. (**A**) Subcellular localization of RAFT1, gephyrin, and control proteins in rat brain fractions (*15*). H, homogenate; P1, crude nuclei; P2, mitochondria and synaptosomes; P3, crude microsomes; S3, cytosol; LP1, postsynaptic densities; LP2, presynaptic membranes and synaptic vesicles; LS2, soluble synaptosomal components, and synapt., synaptophysin. (**B**) Enrichment of RAFT1 in non-nuclear cellular membranes. Subcellular fractions of HeLa cells (*21*) were analyzed by immunoblotting with affinity-purified 782 antibody to RAFT1 (*19*). (**C**) Altered subcellular localization of endogenous RAFT1 in cells expressing the RAFT1 GBD (residues 1010 to 1128). HeLa cells transfected with a mycGBD construct were stained with mouse antibody 9E-10 to myc (red cells, right panel) and rabbit 782 antibody to endogenous RAFT1 (green cells, left panel) (*22*). Cells that are green in the left panel and not red in the right panel serve as controls for the localization of endogenous RAFT1 in HeLa cells in the absence of mycRAFT1 GDB expression. Quantitation of two separate experiments indicated that 64 out of 70 cells expressing mycGBD showed RAFT1 localization similar to that shown. Expression of control myc-tagged proteins did not disrupt RAFT1 localization (*13*). (**D**) Expression in HeLa cells of mycRAFT1 (green) with gephyrin causes mycRAFT1 to appear in large clumps in the cytoplasm. mycRAFT1 was detected with antibody 9E-10 to myc (*22*). Similar results were obtained with COS cells (*13*).

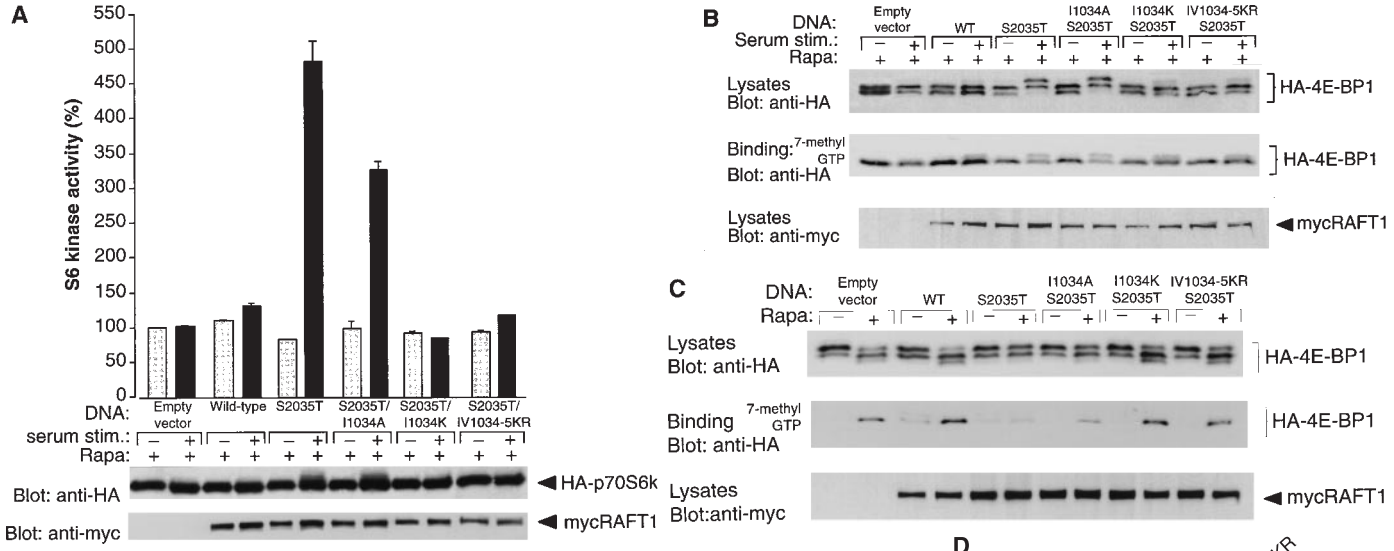

Fig. 4. GBD mutations that disrupt the RAFT1-gephyrin interaction prevent RAFT1-mediated signaling. (**A**) Serum-stimulated $p70^{S6k}$ activation. Quiescent HEK293 cells expressing the indicated mycRAFT1 variants and HA-$p70^{S6k}$ were treated with 10 nM rapamycin for 30 min. Cells were lysed after rapamycin treatment (shaded bars) or after serum stimulation for 30 min (black bars), and S6 kinase activity was determined (*7*). Results are means ± SE for three separate experiments and normalized to the S6 kinase activity in rapamycin-treated cells expressing only $p70^{S6k}$. Expression of $p70^{S6k}$ (top panel) and RAFT1 variants (bottom panel) was monitored with immunoblotting (*23*). (**B**) Serum-stimulated 4E-BP1 phosphorylation. Cells expressing the indicated mycRAFT1 variants and HA–4E-BP1 were treated as in (A). The amount of 4E-BP1 bound to eIF-4E was determined by immunoblotting of proteins interacting with a 7-methyl–guanosine triphosphate (GTP) affinity resin (middle) (*7*). Expression of 4E-BP1 (top) and RAFT1 variants (bottom) was analyzed with immunoblotting (*23*). Results are representative of three separate experiments. (**C**) Phosphorylation of 4E-BP1 in actively growing cells. Twenty-four hours after transfection, HEK293 cells expressing the indicated mycRAFT1 variants and HA–4E-BP1 were treated with 10 nM rapamycin or ethanol vehicle for 30 min. Cells were then lysed and the amount of 4E-BP1 bound to eIF-4E (middle) was determined as in (B). Expression of 4E-BP1 (top) and RAFT1 variants (bottom) was detected with immunoblotting (*23*). Results are representative of four separate experiments. (**D**) The GDB mutations do not impair the capacity of mycRAFT1 to autophosphorylate (middle) or phosphorylate 4E-BP1 (bottom). Kinase assays were done as described (*24*) after immunoprecipitation with 9E-10 antibody to myc. Expression of mycRAFT1 was monitored with immunoblotting (top).

minimal GBD of RAFT1 (amino acids 1010 to 1128) disrupted the normal subcellular localization of RAFT1, causing the protein to appear in clumps dispersed throughout the cytoplasm (Fig. 3C). When mycRAFT1 was expressed in HeLa cells, it was evenly distributed throughout the cytoplasm (Fig. 3D), with an appearance similar to that of endogenous RAFT1 (Fig. 3C). However, when

mycRAFT1 was expressed with gephyrin, it appeared in large aggregates in the cell cytoplasm (Fig. 3D). The glycine receptor, a known gephyrin-binding protein, displays a similar localization when expressed with gephyrin in HEK293 cells (*10*).

Great overexpression of any protein substantially inhibits $p70^{S6k}$ activity and 4E-BP1 phosphorylation (*17*), precluding us from testing the effects of GBD expression on the activity of these downstream signaling molecules. Instead, to determine whether the association with gephyrin is necessary for RAFT1 function, we tested whether RAFT1 mutants incapable of interacting with gephyrin were able to signal to $p70^{S6k}$ and 4E-BP1. We incorporated the GBD mutations into RAFT1 S2035T, a version of the protein that can activate downstream transducers even in the presence of rapamycin because it does not bind the rapamycin-FKBP12 complex (*3*). In quiescent cells treated with rapamycin, serum induces a fivefold increase in $p70^{S6k}$ activity in cells expressing S2035T but not in cells expressing wild-type RAFT1 (Fig. 4A). The rapamycin-resistant function of RAFT1 S2035T depends on its wild-type GBD because the addition of mutations that disrupt gephyrin binding (I1034K or IV1034-5KR) also eliminates its ability to activate $p70^{S6k}$ in the presence of rapamycin (Fig. 4A). RAFT1 I1034A retains partial binding to gephyrin, and the I1034A/S2035T double mutant allowed an intermediate amount of rapamycin-resistant, serum-inducible activation of $p70^{S6k}$ (Fig. 4A).

The RAFT1 mutants deficient in gephyrin binding could not mediate signaling to 4E-BP1, the small translational repressor whose interaction with eIF-4E is blocked by rapamycin-sensitive phosphorylation (*3*). Expression of RAFT1 S2035T having a wild-type or I1034A GBD allowed serum-stimulated, rapamycin-resistant phosphorylation of 4E-BP1. We detected 4E-BP1 phosphorylation in two ways: decreased migration of 4E-BP1 on SDS-PAGE and a decrease in the amount of 4E-BP1 that interacted with eIF-4E (Fig. 4B). Incorporation of the I1034K or IV1034-5KR mutations eliminated the ability of RAFT1 S2035T to signal to 4E-BP1 in the presence of rapamycin (Fig. 4B).

In addition to preventing serum-stimulated 4E-BP1 phosphorylation in quiescent cells, rapamycin treatment causes dephosphorylation of this protein in actively growing cells (*3*). 4E-BP1 was protected from rapamycin-induced dephosphorylation in cells expressing 4E-BP1 with RAFT1 S2035T or I1034A/S2035T (Fig. 4C). In cells expressing only 4E-BP1 or 4E-BP1 with wild-type or S2035T/I1034K RAFT1, rapamycin produced the characteristic signs of 4E-BP1 dephosphorylation (Fig. 4C). The perturbed function of the RAFT1 GBD mutants appears not to be due to an effect of the mutations on RAFT1 kinase activity because the GBD mutants autophosphorylated and phosphorylated 4E-BP1 as efficiently as did the wild-type enzyme (Fig. 4D).

There is increasing awareness of the role translational controls play in many biological phenomena. Signaling pathways that regulate protein synthesis are likely to be important for the translation of mRNAs localized to distinct cellular compartments, such as neuronal dendrites (*18*). In neurons gephyrin is localized to synaptic sites in dendrites (*9*). Our finding that RAFT1 interacts with gephyrin makes RAFT1 an attractive candidate for a regulator of dendritic mRNA translation.

References and Notes

1. K. Savitsky *et al.*, *Science* **268**, 1749 (1995); K. O. Hartley *et al.*, *Cell* **82**, 849 (1995); E. J. Brown *et al.*, *Nature* **369**, 756 (1994); D. M. Sabatini *et al.*, *Cell* **78**, 35 (1994); C. J. Sabers *et al.*, *J. Biol. Chem.* **270**, 815 (1995); M. I. Chiu, H. Katz, V. Berlin, *Proc. Natl. Acad. Sci. U.S.A.* **91**, 12574 (1994); J. Kunz *et al.*, *Cell* **73**, 585 (1993); R. Cafferkey *et al.*, *Mol. Cell. Biol.* **13**, 6012 (1993); D. M. Morrow *et al.*, *Cell* **82**, 831 (1995).
2. T. Jayaraman and A. R. Marks, *J. Biol. Chem.* **268**, 25385 (1993); M. W. Albers *et al.*, *ibid.*, p. 22825; S. N. Sehgal, H. Baker, C. Vezina, *J. Antibiot.* (*Tokyo*) **28**, 727 (1975); J. Heitman, N. R. Movva, M. N. Hall, *Science* **253**, 905 (1991).
3. J. Chung, C. J. Kuo, G. R. Crabtree, J. Blenis, *Cell* **69**, 1227 (1992); C. J. Kuo *et al.*, *Nature* **358**, 70 (1992); E. J. Brown *et al.*, *ibid.* **377**, 441 (1995); L. Beretta *et al.*, *EMBO J.* **15**, 658 (1996); S. R. von Manteuffel *et al.*, *Proc. Natl. Acad. Sci. U.S.A.* **93**, 4076 (1996).
4. G. J. Brunn *et al.*, *Science* **277**, 99 (1997).
5. N. C. Barbet *et al.*, *Mol. Biol. Cell* **7**, 25 (1996).
6. C. T. Keith and S. L. Schreiber, *Science* **270**, 50 (1995).
7. P. E. Burnett *et al.*, *Proc. Natl. Acad. Sci. U.S.A.* **95**, 1432 (1998).
8. The yeast reporter strain Y190, which contains the reporter genes *lacZ* and *HIS3* downstream of binding sequences for GAL4, was sequentially transformed with pPC97 containing the cDNA for RAFT1(944–1338) and a rat hippocampal expression library in pPC86 [P. M. Chevray and D. Nathans, *Proc. Natl. Acad. Sci. U.S.A.* **89**, 5789 (1992)]. Screening of 6.5×10^6 clones yielded one His^+-$LacZ^+$ colony. The rescued library plasmid encoded amino acids 209 to 685 of gephyrin. Truncations and mutations of RAFT1(944–1338) were made with polymerase chain reaction–based mutagenesis techniques.
9. P. Prior *et al.*, *Neuron* **8**, 1161 (1992); J. Kirsch, I. Wolters, A. Triller, H. Betz, *Nature* **366**, 745 (1993).
10. G. Meyer, J. Kirsch, H. Betz, D. Langosch, *Neuron* **15**, 563 (1995); J. Kirsch, J. Kuhse, H. Betz, *Mol. Cell. Neurosci.* **6**, 450 (1995).
11. GST and GST-gephyrin (residues 209 to 685) proteins were expressed in *Escherichia coli* BL21(DE3) and purified with glutathione-agarose [D. B. Smith and K. S. Johnson, *Gene* **67**, 31 (1988)]. Plates (10 cm in diameter) of 80% confluent HEK293 cells were lysed (300 μl per plate) in buffer A [50 mM Hepes-KOH (pH 7.4), 40 mM NaCl, 0.5% Triton X-100, 2 mM EDTA, 1 mM phenylmethylsulfonyl fluoride, aprotinin (5 mg/ml), antipain (1 mg/ml), leupeptin (1 mg/ml), chymostatin (6 mg/ml), and pepstatin A (0.7 mg/ml)] and 100 μl added to 5 μg of GST or GST-gephyrin bound to 20 μl of glutathione-agarose beads. After a 1-hour incubation on ice, the beads were washed three times with buffer A containing 500 mM NaCl. Bound RAFT1 was eluted with 1.25× sample buffer and detected by immunoblotting with 782 antibody to RAFT1 (anti–782-RAFT1) (*19*).
12. HEK293 cells plated on 10-cm dishes were transfected with the calcium phosphate precipitate method with myc-tagged RAFT1 variants (5 μg) and hemagglutinin (HA)–tagged gephyrin(209–685) in pRK5 (5 μg). After 24 to 36 hours, cells were rinsed once with phosphate-buffered saline (PBS) and lysed in 1 ml of ice-cold buffer A (*11*) containing 1.5 mM Na_3VO_4, 50 mM NaF, 10 mM sodium pyrophosphate, and 10 mM sodium β-glycerophosphate. Immune complexes were prepared with 0.5 μl of rabbit antibody to HA (Babco) and 40 μl of protein A–Sepharose and washed three times with buffer A containing 500 mM NaCl. Bound proteins were eluted with 1.25× sample buffer, and RAFT1 was detected by immunoblotting with 9E10 antibody to myc (Calbiochem).
13. D. M. Sabatini and S. H. Snyder, unpublished observations.
14. In situ hybridization was done as described [S. Blackshaw and S. H. Snyder, *J. Neurosci.* **17**, 8074 (1997)] with sense or antisense digoxigenin-labeled RNA probes corresponding to amino acids 209 to 685 of gephyrin or 944 to 1338 of RAFT1 (*13*).
15. Rat brain subcellular fractions were prepared as described [P. E. Burnett *et al.*, *Proc. Natl. Acad. Sci. U.S.A.* **95**, 8351 (1998)]. The quality of the subcellular fractions was monitored by protein immunoblotting of 20 μg of each fraction with antibodies to mGluR1α (Pharmingen), PSD-95 (Santa Cruz), synaptophysin (Boehringer Mannheim), and FKBP12 [L. Walensky *et al.*, *J. Cell Biol.* **141**, 143 (1998)]. The gephyrin [B. T. Kawasaki, K. B. Hoffman, R. S. Yamamoto, B. A. Bahr, *J. Neurosci. Res.* **49**, 381 (1997)] and RAFT1 antibodies (*19*) have been described.
16. D. Watters *et al.*, *Oncogene* **14**, 1911 (1997).
17. Transfection of HA-$p70^{S6k}$ in prk5 (100 ng) with >5 μg of any of several expression vectors encoding a variety of proteins results in less than 30% of the S6 kinase activity obtained when HA-$p70^{S6k}$ (100 ng) is transfected with 10 μg of empty expression vector (*13*).
18. O. Steward and G. A. Banker, *Trends Neurosci.* **15**, 180 (1992); F. B. Gao, *BioEssays* **20**, 70 (1998).
19. D. M. Sabatini *et al.*, *J. Biol. Chem.* **270**, 20875 (1995).
20. Single-letter abbreviations for amino acid residues are as follows: A, Ala; C, Cys; D, Asp; E, Glu; F, Phe; G, Gly; H, His; I, Ile; K, Lys; L, Leu; M, Met; N, Asn; P, Pro; Q, Gln; R, Arg; S, Ser; T, Thr; V, Val; W, Trp; and Y, Tyr.
21. HeLa cells were fractionated [J. Kruppa and D. D. Sabatini, *J. Cell Biol.* **74**, 414 (1977)], 50 μg of each fraction was resolved by SDS–polyacrylamide gel electrophoresis (SDS-PAGE) (6% gels), and RAFT1 was detected with antibody 782 to RAFT1 (*19*).
22. HeLa cells grown on chamber slides were transfected with lipofectamine (Life Technologies) with expression vectors encoding mycGBD (residues 1010 to 1128 of RAFT1) (10 μg); mycRAFT1 (5 μg), and prk5 (5 μg); or mycRAFT1 (5 μg) and gephyrin P1 (5 μg) (*9*). After a 48-hour incubation, the cells were processed for immunofluorescence [L. D. Walensky and S. H. Snyder, *J. Cell Biol.* **130**, 857 (1995)]. Antibodies 9E-10 to myc (2 μg/ml) or 782 to RAFT1 (5 μg/ml) (*19*) were used as the primary antibodies in an overnight incubation at 4°C.
23. Expression constructs of $p70^{S6k}$, 4E-BP1, and RAFT1 were prepared as described (*7*). HEK293 cells were transfected with HA-$p70^{S6k}$ (100 ng) or HA–4E-BP1 (50 ng) alone or with 2 μg of each RAFT1 variant. The total amount of DNA was kept constant at 10 μg with empty pRK5. The cells were incubated overnight, rinsed once with PBS, and placed in medium without fetal bovine serum (FBS) for 30 to 48 hours. Cells were treated with 10 nM rapamycin (Calbiochem) for 30 min. Stimulation with 10% FBS was for 30 min. After treatments, cells were rinsed once with PBS and lysed (*12*). Proteins were resolved by SDS-PAGE (8% gels for $p70^{S6k}$ and 17% gels for 4E-BP1) and detected with immunoblotting.
24. RAFT1 kinase assays were done as described (*7*). The addition to the assays of 1.5 μg of GST-gephyrin (*11*) did not affect RAFT1 autophosphorylation nor was gephyrin a RAFT1 substrate (*13*).

25. We thank T. Morimoto for help with HeLa cell fractionation, A. Lanahan and P. Worley for the rat hippocampal library, and L. Walensky, N. Cohen, and J. Lawler for fruitful discussions. Supported by U.S. Public Health Service grant DA-00266 and Research Scientist Award DA-00074 to S.H.S., and training grant GM-07309 to D.M.S.

6 November 1998; accepted 9 April 1999